AD_____

Award Number: W81XWH-10-1-0982

TITLE: Early Detection of Heterotopic Ossification for Effective Prevention and Treatment

PRINCIPAL INVESTIGATOR: Zijun Zhang, PhD/MD

CONTRACTING ORGANIZATION:
MedStar Health Research Institute
Hyattsville, MD 20782-2031

REPORT DATE: April 2014

TYPE OF REPORT: Final

PREPARED FOR: U.S. Army Medical Research and Materiel Command
Fort Detrick, Maryland 21702-5012

REPORT DOCUMENTATION PAGE

Form Approved
OMB No. 0704-0188

1. REPORT DATE	2. REPORT TYPE	3. DATES COVERED
April 2014	Final	30 Sep 2010- 28 Jan 2014

4. TITLE AND SUBTITLE
Early Detection of Heterotopic Ossification for Effective Prevention and Treatment

5a. CONTRACT NUMBER

5b. GRANT NUMBER
W81XWH-10-1-0982

5c. PROGRAM ELEMENT NUMBER

6. AUTHOR(S)
Zijun Zhang

E-Mail: zijun.zhang@medstar.net

5d. PROJECT NUMBER

5e. TASK NUMBER

5f. WORK UNIT NUMBER

7. PERFORMING ORGANIZATION NAME(S) AND ADDRESS(ES)
MedStar Health Research Institute
Hyattsville, MD 20782-2031

8. PERFORMING ORGANIZATION REPORT NUMBER

9. SPONSORING / MONITORING AGENCY NAME(S) AND ADDRESS(ES)
U.S. Army Medical Research and Materiel Command
Fort Detrick, Maryland 21702-5012

10. SPONSOR/MONITOR'S ACRONYM(S)

11. SPONSOR/MONITOR'S REPORT NUMBER(S)

12. DISTRIBUTION / AVAILABILITY STATEMENT
Approved for Public Release; Distribution Unlimited

13. SUPPLEMENTARY NOTES

14. ABSTRACT

1. Prepared SDF-1 molecular probe for near infrared imaging.
2. Completed animal models of muscle injury; osteotomy; and muscle injury + osteotomy.
3. Performed near infrared imaging of SDF-1 in injured muscles.
4. Isolated muscle derived mesenchymal stem cells from animal models of muscle injury; osteotomy; and muscle injury + osteotomy, and analyzed their osteogenic potential.

15. SUBJECT TERMS

16. SECURITY CLASSIFICATION OF:			17. LIMITATION OF ABSTRACT	18. NUMBER OF PAGES	19a. NAME OF RESPONSIBLE PERSON
a. REPORT	b. ABSTRACT	c. THIS PAGE			USAMRMC
U	U	U	UU	16	19b. TELEPHONE NUMBER *(include area code)*

Table of Contents

INTRODUCTION:

Heterotopic ossification (HO) is a pathological condition where soft tissues, such as muscles, calcify. Clinically, there are several forms of HO. Relevant to orthopaedic traumatology is HO that occurs in elbow [1] and hip [2] as a complication of injury, burn, brain injury or surgery [3, 4, 5]. The prevalence of HO in wartime extremity injuries, particularly after amputation, is as high as 64% [6, 7]. HO can be painful and impair the motions and functions of prostheses and the affected extremities [8]. Prophylactic radiation and medications such as nonsteroidal anti-inflammatory drugs (NSAIDs) are effective [9, 10, 11], but these measures are not without serious side-effects and may be impractical for wartime injuries.

Effective treatments and prevention must precisely target at HO pathogenesis, which has not been fully revealed. A few clinical conditions, however, have been linked to the development of HO. HO gained attention of orthopaedic surgery largely as a complication of hip arthroplasty, which became a common procedure decades ago [12]. Among the risk and predisposing factors summarized from clinical data, spreading bone marrow to the surgical field during reaming femoral canal was speculated [13]. This theory is supported by an animal study, in which HO was successfully induced in rabbits by surgical reaming of femoral medullary canal and intentionally leaving bone debris and marrow materials in the wound [14]. Bone marrow is well-known for containing mesenchymal stem cells (MSCs) and other osteogenic elements [15]. MSCs, however, reside in almost all the tissues for homeostasis and repair. Muscle-derived MSCs (M-MSCs) are capable of multi-lineage differentiation, including osteogenesis [16, 17]. It, therefore, raises a legitimate question about the role of M-MSCs in the development of HO [4, 18].

The molecular biology of HO and fracture healing shares a common process of MSC osteogenesis. In fracture healing or repair of other tissues, MSCs are recruited to the injury site by chemokines. Stem cell-derived factor-1 (SDF-1) is one of the chemokines that are selectively up-regulated by ischemia or injury, such as fracture [19, 20].

CXCR4 is the receptor of SDF-1 and is expressed by stem/progenitor cells in fracture healing [21, 22, 23]. Up-regulation of SDF-1 in local tissues forms a chemokine gradient and attracts CXCR4-expressing stem/progenitor cells for angiogenesis and repair [24]. The local expression of SDF-1 was quantitatively correlated with the volume of new bone formation [25]. The SDF-1/CXCR4 axis for stem/progenitor cell recruitment is critical for fracture healing and could also play an important role in the development of HO, which is resulted from osteogenic differentiation of M-MSCs.

Muscle injury is regarded as a risk factor of HO formation in hip arthroplasty [26]. In the development of HO, subtle muscle injuries could trigger SDF-1 build-up locally and MSC recruitment. This project is based on a hypothesis that the detection of locally increased SDF-1 is indicative of MSC accumulation, preceded tissue ossification i.e. HO development.

Analyses of clinical data have long noticed the potential roles of bone fracture or osteotomy and local muscle injury in the development of HO [2]. This study was designed to investigate whether muscle and bone injuries differentially affect the osteogenic potential of M-MSCs and contribute to the pathogenesis of HO. In reaction to bone or muscle injury, local accumulation of SDF-1 may be different. Since the concentrations of SDF-1 correlate with the amount of MSC recruitment, it may serve as an indicator of potential HO development in the injured muscles. This study intended to explore a correlation between SDF-1 accumulation and HO development, as implied by the osteogenic potential of M-MSCs.

This project aimed to 1) link local SDF-1 and stem cell recruitment with HO development; 2) distinguish the contribution of bone and muscle injury to the pathogenesis of HO; 3) explore the possibility of molecular imaging as a tool for early diagnosis of HO.

BODY:

To establish an animal model of HO and make molecular probe of SDF-1 were the priorities of this project. During the first 6 months of this project, we performed a series of experiments to prepare a fluorescent conjugated antibody of SDF-1 for near infrared imaging **(Task 1)**.

1) Selection of a SDF-1 antibody from several commercial suppliers. After literature review and online research, we chose two antibodies that react with rat/mouse SDF-1 for further evaluation. They were rabbit anti SDF-1 antibody produced by GeneTex (Cat No GTX45117) and goat anti SDF-1 antibody produced by Santa Cruz Biotechnology (Cat No SC-6193).

2) The specificity and sensitivity of the two antibodies were tested by reactions with SDF-1 protein in serial dilutions, using enzyme-linked immunosorbent assay (ELISA). The experiment was done in triplicate. In general, the readings (reaction of SDF-1 protein with antibody) of the GeneTex product were slightly higher than that using the antibody produced by Santa Cruz Biotechnology.

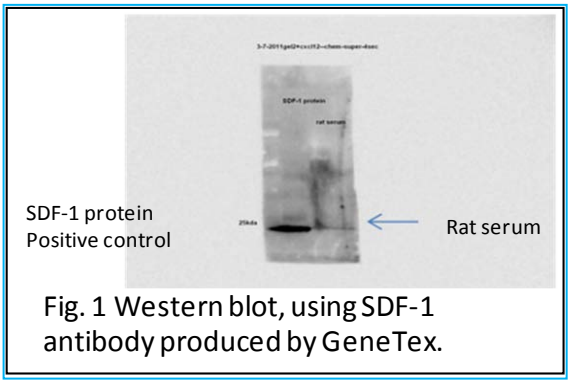

Fig. 1 Western blot, using SDF-1 antibody produced by GeneTex.

3) The specificity and sensitivity of SDF-1 antibody produced by GeneTex was further tested in rat serum, which contains SDF-1 at a very low concentration, with western blot. Pure SDF-1 protein was used as a positive control. A band in corresponding to SDF-1 protein was detected in rat serum with the SDF-1 antibody produced by GeneTex (Figure 1).

Based on the tests of specificity and sensitivity, SDF-1 antibody produced by GeneTex (Cat No GTX45117) was selected to make the molecular probe for near infrared imaging of SDF-1.

We planned to label the SDF-1 antibody with a near infrared fluorochrome, cypate, made by Dr. Achilefu's laboratory at Washington University School of Medicine. Due to personnel changes, however, cypate supply was interrupted. Instead, we decided to label the antibody with a commercially available near infrared fluorochrome—Alexa Fluor 750 (Life Technologies). This fluorescence is equivalent to cypate and had been applied for animal studies previously [27].

Alexa Fluor 750 and SDF-1 antibody were conjugated using a SAIVI Rapid Antibody Labeling Kit (Invitrogen). The degree of labeling (DOL), which was calculated according to protein absorbance and fluorescent absorbance, of the resultant molecular probe of SDF-1 was

2.45. This DOL was in the range recommended by the manufacturer. This result marked a **Milestone** of this project: SDF-1 antibody tagged with near infrared fluorochrome.

An animal protocol for this study was approval by Saint Louis University IACUC and ACURO **(Task 2a)**. According to the protocol, a pilot study was performed using 5 rats **(Task 2b)**. The purpose of this pilot study was to familiarize the hip topographic anatomy of rats and test the animal tolerance to the proposed surgery. A commonly used HO model is to induce ossification by ischemic muscle injury [28]. Under anesthesia, both rat hips were prepared for surgery. Gluteus medius was exposed through an incision around the hip. On the experimental side, the muscle was clamped (2 steps) with a pair of hemostatic forceps for 5 minutes to cause ischemic muscle injury. Sham surgery---without ischemic damage---was performed on the opposite hip for controls. Tissue ossification was found at 10 weeks by radiography.

The results of this pilot study led us to reconsider the animal model for this study. Rats were proposed for the creation of a HO model, primarily because of its relatively larger body size than mice. Surgical dissection of muscles around the hip in rats would be much easier than in mice. After the pilot study, we felt that the surgical dissection of hip muscles was not as challenging as originally thought. We were confident that this muscle injury model could be surgically produced in mice to test the original study hypothesis. The following justification was used to support switching from rats to mice for this study:

1) An important part of this study was to map SDF-1 in HO models, using near infrared imaging. This imaging method was much more commonly used for mice than rats. The imaging settings for mice were well defined and the technicians operate the imaging instrument were more familiar with mouse imaging than imaging other species. Using mice for this study would avoid a learning curve in imaging.

2) The body size of mice would not be a problem surgically and, in fact, was a great advantage for molecular imaging. Due to their small body size, mice would require injecting much less antibody-probe for imaging than using rats. Using mice, this project would save on the expense of molecular probe and enable us to test more conditions in HO development. Near infrared imaging had been used on the knee joints of mice [29]. Those data and protocols would be valuable references for this project.

3) We planned to isolate mesenchymal stem cells from the injured muscles. Protocols were readily available for isolation of mesenchymal stem cells from mouse muscles [30].

The PI, Zijun Zhang, moved to MedStar Health Research Institute/MedStar Union Memorial Hospital in September 2011. We used this opportunity revised the animal protocol to use mice for HO development. The grant was transferred from Saint Louis University to MedStar Health Research Institute in April 2012 **(Task 2c)**.

A revised animal protocol was approved by MedStar Health Research Institute IACUC and the ACURO subsequently **(Task 2d)**.

Task 2e: SDF-1 antibody (GeneTex, Cat No GTX45117) was conjugated with near infrared fluorochrome, Alexa Fluor 750 (Life Technologies), using the procedure previously developed. The degree of labeling (DOL) of the resultant molecular probe of SDF-1 was 1.981, which was in the range recommended by the manufacturer.

Alexa Fluor 750-labeled SDF-1 antibody (5ng/15µl) was injected into a piece of muscle collected from a mouse. The antibody injected muscle and a piece of muscle without injection were placed in a petri dish filled with phosphate buffered saline and imaged with In Vivo Image System. The fluoresce-conjugated SDF-1 antibody was clearly detected (Figure 2). This confirmed the success of labeling of SDF-1 antibody and the conditions of imaging.

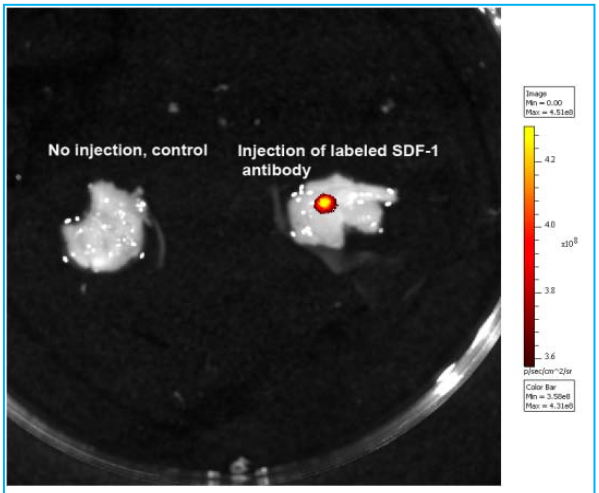

Fig 2. Testing Alexa Fluor 750 conjugated SDF-1 antibody. The antibody injected into muscles was detected by near infrared imaging (red).

Bone fracture or osteotomy and muscle injury have long been identified as risk factors of HO [2]. In this study ischemic injury of gluteus maximus and medius, and osteotomy of great trochanter of femur were applied separately or in combination to mice.

A total of 75 C57BL/6 mice (Charles River), male, 8 weeks old, were used for this study. Animal surgery and care were conducted at the animal facilities of MedStar Health Research Institute. The mice were anesthetized with intraperitoneal injection of a cocktail (Ketamine 80mg/kg and Xylazine 10mg/kg). After skin preparation, an incision about 2 cm was made over the right hip to expose gluteus maximus and medius. Each animal was randomly to receive one of three surgical procedures:

1) Muscle injury (Group M): The gluteus maximus and gluteus medius were gently dissected about 5 mm from great trochanter. Two pairs of hemostatic forceps were used to pinch the muscles in parallel (2-3 mm apart). To be consistent in muscle damage, the hemostatic forceps were clamped two steps at the same time for 5 minutes.

2) Osteotomy (Group O): A powered bur was used to cut the great trochanter from the junction with femoral shaft. The great trochanter was then loosely reattached with a stitch (Vicryl 5.0).

3) Muscle injury and osteotomy (Group M+O): After muscle injury of gluteus maximus and gluteus medius was performed as previously described, osteotomy of great trochanter was conducted as mentioned in group O.

The wound was closed with continuous subcutaneous sutures. The animals were returned to cages without immobilization. Animals were allowed to use the operated extremity *ad lib*.

Post-surgery analgesia and antibiotics were given for the first 3 and 7 days, respectively. In each study group, 3-8 mice were sacrificed at days 1, 3, 5 and 10 (see Table 1 for animal distribution).

Table 1. Animal distribution in groups and the time-points of sacrifice

	M group	O group	M+O group
Day1	5	5	5
Day3	7(3)	8(3)	8(3)
Day5	6(3)	6(3)	3(3)
Day10	3(3)	3(3)	3(3)

Note: number of animals imaged in bracket.

On the day of sacrifice, three mice in each study group at days 3, 5, and 10 were injected with 10 µg SDF-1 antibody conjugated with Alexa Fluor 750 in 150 µl saline, via tail vein. Mice were sacrificed in four hours after injections of SDF-1 antibody.

The gluteus maximus and medius on the operated hips were dissected with aseptic techniques and placed individually in 6-well plates, covered with phosphate buffered saline. The dissected muscles were imaged at Molecular Imaging Laboratory, Howard University, directed by Dr. Paul Wang. The intensity of near infrared imaging was calculated for comparisons among the groups. This was a study **Milestone**: imaging SDF-1 distribution in HO.

Task 2f: After imaging, the muscle samples were minced and digested in 1% collagenase (type I, Life Technologies), as described by Nesti et al. [30, 31], for M-MSC isolation. The collected cells were plated at a density of 3,000 cells/cm^2 and cultured with Dulbecco's Modified Eagle Medium (DMEM, Life Technologies), supplemented with 10% fetal bovine serum, with 5% carbon dioxide in the air at 37ºC. The cells were passaged at 70% confluent and used at passage 3 for this study.

1) Flow cytometry: M-MSCs isolated from gluteus maximus and gluteus medius in M, O and M+O groups at day 10 were incubated with fluorescence-labeled antibodies of CD73, CD90 and CD105. According to the recommendation of International Society for Cellular Therapy, CD73, CD90 and CD105 are the common MSC cell surface markers [32]. Flow cytometry was also performed on myogenic progenitor marker CD56 [33] and muscle-derived MSC marker CD140 (platelet-derived growth factor receptor alpha PDGFRa) [34]. The data were analyzed with Flow-Jo.

2) Osteogenic differentiation of M-MSCs: At passage 3, M-MSCs were plated in 48-well culture plates and cultured in an osteogenic medium, which was based on DMEM and supplemented with 10% fetal bovine serum, 10 mM β-glycerophosphate, 100 nM dexamethasone, and 50µg/ml ascorbate, for 3 weeks. M-MSCs were also cultured in regular tissue culture medium for experimental controls. In each group and at each time point, M-MSCs from 3 animals were plated. M-MSCs from the same animal were plated in duplicate (see Figure 7 for plate layout). The medium was changed twice a week. After 3 weeks, a portion of the cultures were fixed with 4% paraformaldehyde and stained with Alizarin red. The staining was viewed under a microscope and imaged.
   Osteogenesis of M-MSCs was also quantified, according to Alizarin red stain of matrix mineralization (Millipore). Briefly, after Alizarin red staining, 10% acetic acid

was added into each well of tissue culture plates and incubated for 30 minutes. Cells and acetic acid were collected and heated to 85°C for 10 minutes. After cooled on ice for 5 minutes, the slurry was centrifuged at 20,000g for 15 minutes. The supernatant (400 μl) was transferred to a new tube and neutralized the pH within the range of 4.1 - 4.5. Samples (150 μl) and standards were added to an opaque-walled, transparent bottom 96-well plate and read at OD405 with a microplate reader.

3) Quantification of the expression of osteogenic genes with real-time PCR (polymerase chain reaction): M-MSCs, cultured in osteogenic and control medium, were collected for RNA isolation. RNA was extracted using the TRIzol method. Using the iScript™ Reverse Transcription Supermix for RT-qPCR (Bio-Rad Laboratories), 2.5 μg of total RNA was reverse-transcribed and the products of reverse-transcription were treated with RNase H before storage at –20ºC. Real-time PCR was performed on a CFX Connect™ Real-Time PCR Detection System (Bio-Rad Laboratories). Using Sybr® green PCR Master Mix reagents (Bio-Rad Laboratories), each reaction mixture consisted of 12.5 μl SYBR green PCR reagent, 2.5 μl of 1:50 diluted reverse transcription product, optimized volume of 5 mM primers and DEPC-treated water, for a total volume of 25 μl. No-template and no-reverse transcription reactions were included in each PCR plate as negative controls. The housekeeping gene 18s was used as an internal standard in each PCR plate. After 10 minutes at 95ºC, the PCR amplification was performed for 40 cycles; each cycle consisted of amplification at 95ºC for 50 seconds and 65ºC for 30 seconds. Amplification efficiency of > 90% was required for further processing of the data. Each reaction was performed in triplicate. The cycle at which the fluorescent level was statistically above the background was defined as the threshold cycle (Ct). The Ct values of the gene under investigation were first normalized, as ΔCt, by subtraction of the Ct value of 18s. The relative expression of the gene under investigation (ΔΔCt) was a subtraction of the ΔCt of this gene in M-MSCs cultured in an osteogenic medium from that in the control medium. Quantified expression of the gene was calculated as $2^{-\Delta\Delta Ct}$. Osteogenic genes included type I collagen, osteocalcin and Runx2. Primers were supplied by Integrated DNA Technologies, Coralville, IA.

Statistical analysis: Data of near infrared imaging, flow cytometry, Alizarin red quantification and quantitative PCR expressed as mean ± standard deviation. The cell surface marker expression and osteogenic capacities of M-MSCs among M, O and M+O groups, at different time-points, were comparatively analyzed with ANOVA, followed with *post hoc* Tukey's test. Significance was set as $p<0.05$.

Results:

1) Near infrared imaging of gluteus maximus and medius:

Some groups of muscle samples showed weak fluorescent signals, most likely due to leakage of intravenously injected antibody. No significant differences in average fluorescent intensity of gluteus maximus and medius were detected among the M, O and M+O groups ($p > 0.05$). Figure 3A shows images of muscle samples harvested from the mice of experimental groups M, O and M+O at 3 days post surgery. The fluorescence appeared uniformly through the entire muscle mass. The fluorescent areas and intensities among the three groups were not

significantly different. Muscles in the O group were not injured during the surgery and had reduced fluorescent densities, comparing with the M and M+O groups. However, the difference was not significant ($p>0.05$, Fig 3B).

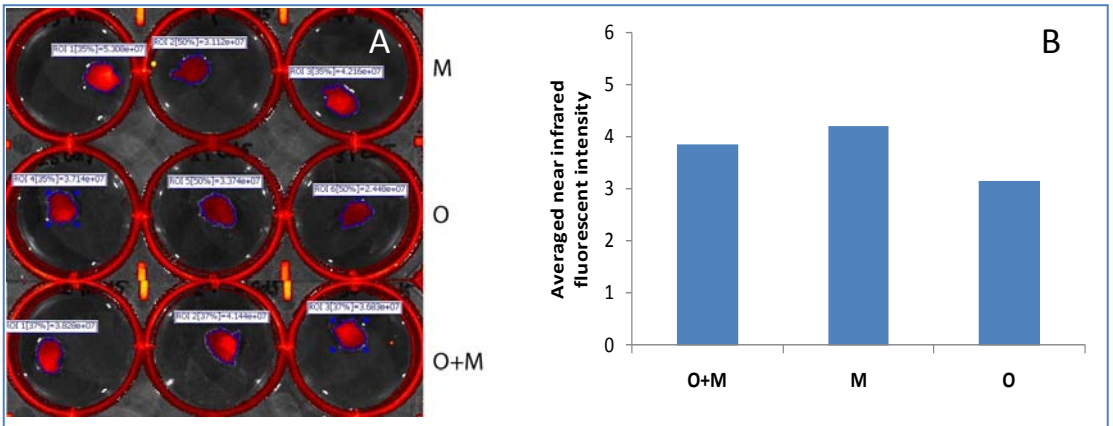

Figure 3. Near infrared images (A) and quantified intensity (B) of gluteus maximus and medius taken from the mice of experimental groups M, O, and M+O at day 3

2) Cell surface marker profiles of M-MSCs from M, O and M+O groups:

The percentages of the expression of cell surface markers in M-MSC populations are listed in Table 2. In general, M-MSCs isolated from M, O and M+O groups (day 10) had similar expressions profiles of common MSC surface markers, except the expression of CD90 was lower in the O and M+O groups than in the M group.

Table 2. Expression of cell surface markers by M-MSCs from M, O, and M+O groups

	Md10	Od10	M+Od10
CD73	84.1	77.9	84.8
CD90	70.5	28.9	25.7
CD105	83.1	84.0	92.8
CD56	81.5	54.6	35.0
CD140	48.3	84.8	91.4

CD56, representing myogenic progenitors, was highly expressed in M-MSCs isolated from M group (day 10), as compared with O and M+O groups (day 10) ($p<0.05$).

CD140, also known as platelet-derived growth factor receptor α (PDGFRα), is a specific marker of muscle derived MSCs. Among the three experimental groups, CD140 was expressed the highest in M-MSCs of the M+O group, followed by the O group and M group ($p<0.05$). Expression of each CD marker by the three groups of M-MSCs is also shown in graph (Figure 4).

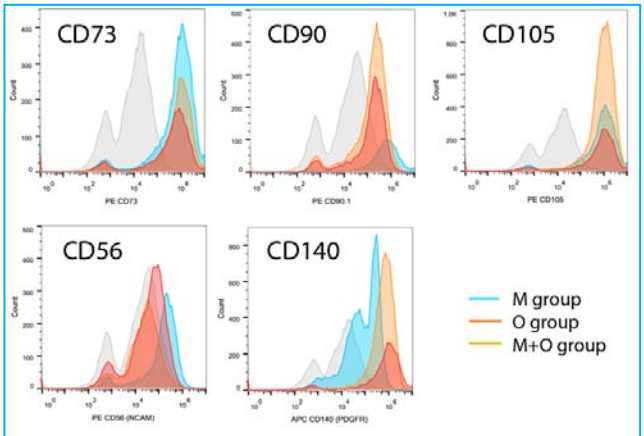

Fig 4. Flow cytometry of CD73, CD90, CD105, CD56 and CD140 in M-MSCs derived from groups M, O, and M+O at day 10. Controls show in gray.

3) The expression of osteogenic genes by M-MSCs in M, O and M+O groups:

For M-MSCs harvested on 1 day post surgery, gene expression of type I collagen, osteocalcin and Runx2 was not significantly different among M, O and M+O groups (Figure 5). In O group, M-MSCs that harvested on days 3, 5 and 10 moderately increased the expression of type I collagen over the time, comparing with the corresponding time-points in M group. Other osteogenic genes such as Runx2 and osteocalcin, however, were not up-regulated in the M-MSCs of both O and M groups. Notably, the expression of type I collagen, Runx2 and osteocalcin by M-MSCs of M+O group harvested on days 3, 5 and 10 was significantly increased, compared with the corresponding ones in M and O groups. Furthermore, the expression of type I collagen, Runx2 and osteocalcin by M-MSCs of M+O group gradually increased over the harvesting time from day 1 to day 10.

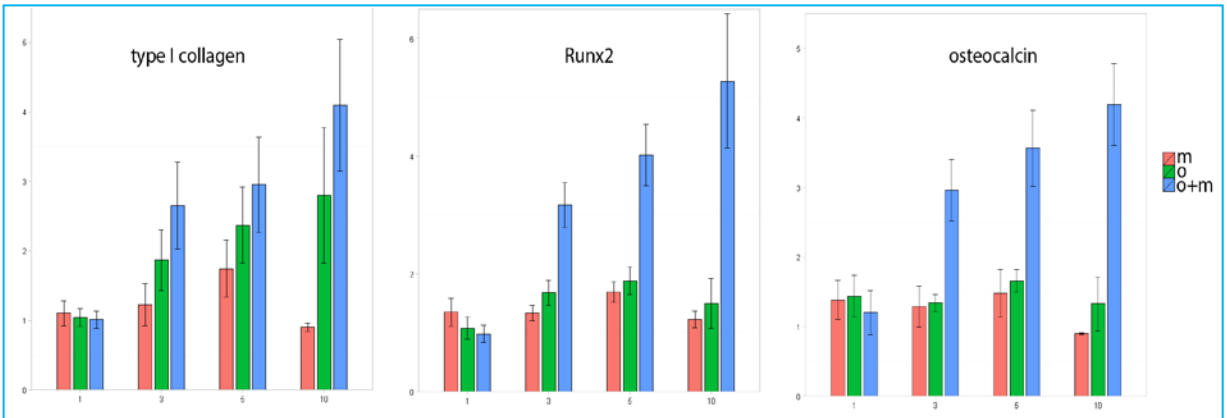

Fig 5. Quantitative expression of osteogenic genes by M-MSCs derived from gluteus maximus and medius of M, O and M+O groups

4) Osteogenesis of M-MSCs in M, O and M+O groups:

After cultured in an osteogenic medium for 3 weeks, M-MSCs derived from gluteus maximus and medius in the groups of M, O and M+O at days 1, 3, 5, and 10 showed varied

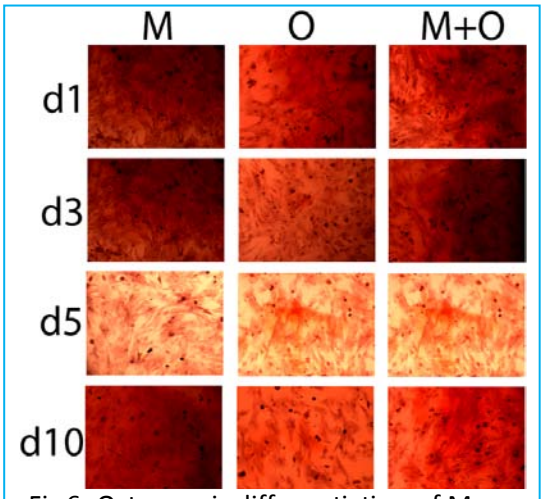

Fig 6. Osteogenic differentiation of M-MSCs in osteogenic cultures (Alizarin red staining)

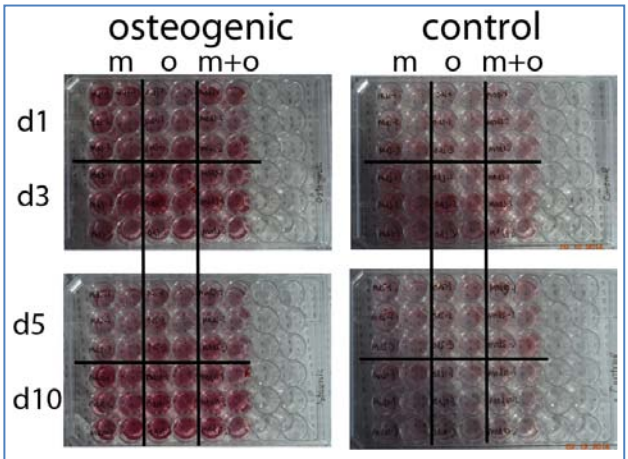

Fig 7. M-MSCs isolated from M, O, and M+O groups at different time-points cultured in osteogenic medium and control (regular) medium for 3 weeks. After stained with Alizarin Red, osteogenic differentiation of M-MSCs was detected, showing in red, in osteogenic, but not control, cultures.

degrees of osteogenesis. Figure 6 shows representing areas stained with Alizarin red in each group. View of the tissue culture plates also demonstrated various degrees of osteogenic differentiation---stained red with Alizarin Red--- of those M-MSCs in the osteogenic cultures, while those cells cultured in control (regular) medium were only faintly stained (Figure 7).

Quantification of Alizarin Red staining in the osteogenic cultures confirmed a significant increase of osteogenic differentiation by the M-MSCs of O and O+M groups harvested at day 10 (Figure 8).

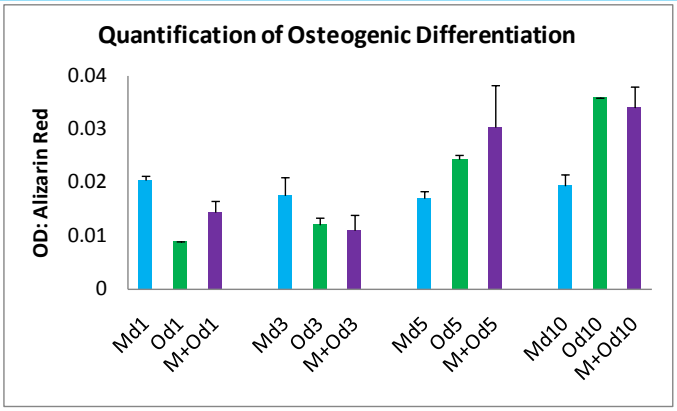

Fig 8. Quantification of Alizarin Red staining of osteogenic differentiated M-MSCs by spectrophotometry. Od10 and M+Od10 had significantly increased osteogenic differentiation, compared with Md10.

KEY RESEARCH ACCOMPLISHMENTS:

1) Synthesis of molecular probe of SDF-1.
2) Near infrared imaging of muscles *de novo*.
3) Animal surgery of muscle injury and osteotomy.
4) Isolation and characterization of M-MSCs isolated from M, O and M+O groups.
5) Evaluation of the osteogenic potential of M-MSCs in M, O and M+O groups.

REPORTABLE OUTCOMES:

1) Established a protocol of SDF-1 antibody labeling and near infrared imaging of injured muscles *de novo*.
2) Mouse models of muscle injury and osteotomy around hip for studying HO.
3) In this animal study, molecular imaging of SDF-1 showed no difference among M, O and M+O groups.
4) M-MSCs isolated from M, O and M+O groups showed differences in cell surface marker profile and osteogenic differentiation.
5) The increased osteogenesis by M-MSCs isolated from M+O group at day 10 was consistently supported by the expression of osteogenic genes and alizarin red staining in osteogenic cultures. It also coincided with an increased subpopulation of CD140 (a marker of muscle-derive MSCs) positive cells and a reduced subpopulation of CD56 (a marker of myogenic progenitors) positive cells in the M-MSCs of M+O group (day 10).

CONCLUSION:

We successfully executed the three phases of the project: 1) imaging SDF-1 in the muscles; 2) creation of mouse HO models with muscle injury, osteotomy, and combined muscle injury and osteotomy; 3) investigation of osteogenic potential of M-MSCs in three animal models.

We proved the concept of molecular imaging of SDF-1 in injured muscles. In this study, we detected no differences in SDF-1 imaging of gluteus maximus and medius among the M, O and M+O groups. It could be, however, due to close proximity of the injured muscles and the

osteotomy sites in mice. A good separation of the injured muscles and osteotomy sites with microsurgical techniques, which are more precise and less invasive than the surgical techniques used in this study, may help better localization of SDF-1 on near infrared images. We still believe that molecular imaging could not only reveal the fundamental pathology of HO but also be translated to the clinic for early detection of HO.

We performed surgery on mice for M, O and M+O models. The animal study provided unique insight of the pathogenesis of HO, specifically the effects of muscle and bone injury. The subsequent analyses of M-MSCs derived from M, O and M+O groups demonstrated that muscle injury, osteotomy and the combination of the two differentially influenced the osteogenic potential of M-MSCs.

M-MSCs isolated in this study, like MSC populations in any other studies, were heterogenic. By characterization of the expression profile of cell surface markers, we demonstrated that M-MSCs derived from M, O and M+O groups consisted of varied subpopulations, which may directly relate to osteogenic potential and the development of HO. Among the three surgical models, the M-MSCs isolated from the M group contained more myogenic progenitors and the M-MSCs in the O and M+O groups had more muscle-derived MSCs. Expression of osteogenic genes by M-MSCs in osteogenic culture was significantly increased in M+O groups, particularly at day 10. Measurements of matrix mineralization indicated that M-MSCs of the O and M+O groups (day 10) had increased osteogenic differentiation. Collectively, the data suggest that muscle injury alone does not increase the osteogenic potential of M-MSCs, possibly due to a higher percentage of myogenic progenitors in total M-MSC population. On the other hand, bone injury (osteotomy) alone or in combination with muscle injury increased the proportion of muscle-derived MSCs in the total population of M-MSCs and the osteogenic potential of M-MSCs. This is consistent with a recently published study, in which muscle injury alone failed to induce HO [35]. But muscle injury and the application of a low dose of BMP-2 (bone morphogenetic protein-2), which could not induce ossification alone, induced robust HO. In our models, osteotomy and the followed bone healing process might have created a critical environment for HO development, including increased osteogenic growth factors such as BMP in the surrounding tissues---gluteus maximus and medius in this study. Muscle injury might have initiated recruitment of MSCs. M+O model could delivered a combination of enhanced MSC recruitment to the injured muscles and active osteogenic environment in the injured muscles---a condition in favor of HO formation.

Limitation of this study: This study was focused on the early molecular events of HO development. Although osteogenic differentiation of M-MSCs is the fundamental cellular pathway of HO, there are other pathological events involve in the formation of HO in soft tissues, such as muscles. Findings of this study such as differences in proportions of myogenic progenitors and muscle-derived MSCs in the entire population of M-MSCs in M, O, and M+O groups may hold a key of HO pathogenesis. This study, however, was limited to offer further causative explanation on this phenomenon. Advantages of animal models include providing well-controlled experimental conditions. Rodents, however, are superior to human in terms of bone formation. These factors should take into consideration in interpreting the results of this study.

Future study: The discrepancies of osteogenic potential in M-MSCs derived from M, O and M+O surgical models will guide further investigations into the effects of muscle and bone injury on osteogenic tissue environment. The expression of osteogenic growth factors such as BMP and TGFβ in the muscles of M, O and M+O models will provide critical information about

the involvement of bone and muscle injury in the development of HO. The altered proportions of myogenic progenitors and muscle-derived MSCs in the M-MSCs of M, O and M+O groups will lead to further examinations of the subpopulations of M-MSCs in detail, to advance our understanding of M-MSCs in HO.

REFERENCES:

1. Lee EK, Namdari S, Hosalkar HS, Keenan MA, Baldwin KD. Clinical results of the excision of heterotopic bone around the elbow: a systematic review. J Shoulder Elbow Surg. 2013;22(5):716-22.
2. Cohn RM, Schwarzkopf R, Jaffe F. Heterotopic ossification after total hip arthroplasty. Am J Orthop (Belle Mead NJ). 2011;40(11):E232-5.
3. Nauth A, Giles E, Potter BK, Nesti LJ, O'Brien FP, Bosse MJ, Anglen JO, Mehta S, Ahn J, Miclau T, Schemitsch EH. Heterotopic ossification in orthopaedic trauma. J Orthop Trauma. 2012;26(12):684-8.
4. Nelson ER, Wong VW, Krebsbach PH, Wang SC, Levi B. Heterotopic ossification following burn injury: the role of stem cells. J Burn Care Res. 2012;33(4):463-70.
5. Sakellariou VI, Grigoriou E, Mavrogenis AF, Soucacos PN, Papagelopoulos PJ. Heterotopic ossification following traumatic brain injury and spinal cord injury: insight into the etiology and pathophysiology. J Musculoskelet Neuronal Interact. 2012;12(4):230-40.
6. Forsberg JA, Pepek JM, Wagner S, Wilson K, Flint J, Andersen RC, Tadaki D, Gage FA, Stojadinovic A, Elster EA. Heterotopic ossification in high-energy wartime extremity injuries: prevalence and risk factors. J Bone Joint Surg Am. 2009;91(5):1084-91.
7. Potter BK, Burns TC, Lacap AP, Granville RR, Gajewski DA. Heterotopic ossification following traumatic and combat-related amputations. Prevalence, risk factors, and preliminary results of excision. J Bone Joint Surg Am. 2007;89(3):476-86.
8. Owens BD, Wenke JC, Svoboda SJ, White DW. Extremity trauma research in the United States Army. J Am Acad Orthop Surg. 2006;14(10 Spec No.):S37-40.
9. Balboni TA, Gobezie R, Mamon HJ. Heterotopic ossification: Pathophysiology, clinical features, and the role of radiotherapy for prophylaxis. Int J Radiat Oncol Biol Phys. 2006;65(5):1289-99.
10. Chao ST, Joyce MJ, Suh JH. Treatment of heterotopic ossification. Orthopedics. 2007;30(6):457-64;
11. Macfarlane RJ, Ng BH, Gamie Z, El Masry MA, Velonis S, Schizas C, Tsiridis E. Pharmacological treatment of heterotopic ossification following hip and acetabular surgery. Expert Opin Pharmacother. 2008;9(5):767-86.
12. Shaffer B. A critical review. Heterotopic ossification in total hip replacement. Bull Hosp Jt Dis Orthop Inst. 1989;49(1):55-74.
13. Pavlou G, Salhab M, Murugesan L, Jallad S, Petsatodis G, West R, Tsiridis E. Risk factors for heterotopic ossification in primary total hip arthroplasty. Hip Int. 2012;22(1):50-5.
14. Tannous O, Stall AC, Griffith C, Donaldson CT, Castellani RJ Jr, Pellegrini VD Jr. Heterotopic bone formation about the hip undergoes endochondral ossification: a rabbit model. Clin Orthop Relat Res. 2013;471(5):1584-92.

15. Post S, Abdallah BM, Bentzon JF, Kassem M. Demonstration of the presence of independent pre-osteoblastic and pre-adipocytic cell populations in bone marrow-derived mesenchymal stem cells. Bone. 2008;43(1):32-9.
16. Lee JY, Qu-Petersen Z, Cao B, Kimura S, Jankowski R, Cummins J, Usas A, Gates C, Robbins P, Wernig A, Huard J. Clonal isolation of muscle-derived cells capable of enhancing muscle regeneration and bone healing. J Cell Biol. 2000;150(5):1085-100.
17. Oishi T, Uezumi A, Kanaji A, Yamamoto N, Yamaguchi A, Yamada H, Tsuchida K. Osteogenic differentiation capacity of human skeletal muscle-derived progenitor cells. PLoS One. 2013;8(2):e56641.
18. Wosczyna MN, Biswas AA, Cogswell CA, Goldhamer DJ. Multipotent progenitors resident in the skeletal muscle interstitium exhibit robust BMP-dependent osteogenic activity and mediate heterotopic ossification. J Bone Miner Res. 2012;27(5):1004-17.
19. Pillarisetti K, Gupta SK. Cloning and relative expression analysis of rat stromal cell derived factor-1 (SDF-1)1: SDF-1 alpha mRNA is selectively induced in rat model of myocardial infarction. Inflammation. 2001;25(5):293-300.
20. Tögel F, Isaac J, Hu Z, Weiss K, Westenfelder C. Renal SDF-1 signals mobilization and homing of CXCR4-positive cells to the kidney after ischemic injury.Kidney Int. 2005;67(5):1772-84.
21. Granero-Moltó F, Weis JA, Miga MI, Landis B, Myers TJ, O'Rear L, et al. Regenerative effects of transplanted mesenchymal stem cells in fracture healing. Stem Cells 2009;27(8):1887-98.
22. Kucia M, Ratajczak J, Reca R, Janowska-Wieczorek A, Ratajczak MZ. Tissue-specific muscle, neural and liver stem/progenitor cells reside in the bone marrow, respond to an SDF-1 gradient and are mobilized into peripheral blood during stress and tissue injury. Blood Cells Mol Dis. 2004;32(1):52-7.
23. Otsuru S, Tamai K, Yamazaki T, Yoshikawa H, Kaneda Y. Bone marrow-derived osteoblast progenitor cells in circulating blood contribute to ectopic bone formation in mice. Stem Cells. 2008;26:223-34.
24. Kucia M, Reca R, Miekus K, Wanzeck J, Wojakowski W, Janowska-Wieczorek A et al. Trafficking of normal stem cells and metastasis of cancer stem cells involve similar mechanisms: pivotal role of the SDF-1-CXCR4 axis. Stem Cells. 2005;23:879-94.
25. Kitaori T, Ito H, Schwarz EM, Tsutsumi R, Yoshitomi H, Oishi S et al. Stromal cell-derived factor 1/CXCR4 signaling is critical for the recruitment of mesenchymal stem cells to the fracture site during skeletal repair in a mouse model. Arthritis Rheum. 2009;60(3):813-23.
26. Schneider DJ1, Moulton MJ, Singapuri K, Chinchilli V, Deol GS, Krenitsky G, Pellegrini VD Jr. The Frank Stinchfield Award. Inhibition of heterotopic ossification with radiation therapy in an animal model. Clin Orthop Relat Res. 1998;(355):35-46.
27. Ushiki T, Kizaka-Kondoh S, Ashihara E, Tanaka S, Masuko M, Hirai H, Kimura S, Aizawa Y, Maekawa T, Hiraoka M. Noninvasive tracking of donor cell homing by near-infrared fluorescence imaging shortly after bone marrow transplantation. PLoS One. 2010;5(6):e11114.
28. Rumi MN, Deol GS, Singapuri KP, Pellegrini VD Jr. The origin of osteoprogenitor cells responsible for heterotopic ossification following hip surgery: an animal model in the rabbit. J Orthop Res. 2005;23(1):34-40.

29. Gompels LL, Madden L, Lim NH, Inglis JJ, McConnell E, Vincent TL, Haskard DO, Paleolog EM. In vivo fluorescence imaging of E-selectin: quantitative detection of endothelial activation in a mouse model of arthritis. Arthritis Rheum. 2011;63(1):107-17.
30. Gharaibeh B, Lu A, Tebbets J, Zheng B, Feduska J, Crisan M, Péault B, Cummins J, Huard J. Isolation of a slowly adhering cell fraction containing stem cells from murine skeletal muscle by the preplate technique. Nat Protoc. 2008;3(9):1501-9.
31. Nesti LJ, Jackson WM, Shanti RM, Koehler SM, Aragon AB, Bailey JR, Sracic MK, Freedman BA, Giuliani JR, Tuan RS. Differentiation potential of multipotent progenitor cells derived from war-traumatized muscle tissue. J Bone Joint Surg Am. 2008;90(11):2390-8.
32. Dominici M1, Le Blanc K, Mueller I, Slaper-Cortenbach I, Marini F, Krause D, Deans R, Keating A, Prockop Dj, Horwitz E. Minimal criteria for defining multipotent mesenchymal stromal cells. The International Society for Cellular Therapy position statement. Cytotherapy. 2006;8(4):315-7.
33. Agley CC1, Rowlerson AM, Velloso CP, Lazarus NR, Harridge SD. Human skeletal muscle fibroblasts, but not myogenic cells, readily undergo adipogenic differentiation. J Cell Sci. 2013;126(Pt 24):5610-25.
34. Uezumi A1, Fukada S, Yamamoto N, Takeda S, Tsuchida K.Mesenchymal progenitors distinct from satellite cells contribute to ectopic fat cell formation in skeletal muscle. Nat Cell Biol. 2010;12(2):143-52.
35. Liu X, Kang H, Shahnazari M, Kim H, Wang L, Larm O, Adolfsson L, Nissenson R, Halloran B. A novel mouse model of trauma induced heterotopic ossification. J Orthop Res. 2013 Oct 17 [Epub ahead of print]

APPENDICES:
N/A